DigiForests: A Longitudinal LiDAR Dataset for Forestry Robotics

Meher V. R. Malladi*[1] Nived Chebrolu*[2] Irene Scacchetti[1] Luca Lobefaro[1]
Tiziano Guadagnino[1] Benoît Casseau[2] Haedam Oh[2] Leonard Freißmuth[3] Markus Karppinen[4]
Janine Schweier[5] Stefan Leutenegger[3] Jens Behley[1] Cyrill Stachniss[1,2,6] Maurice Fallon[2]

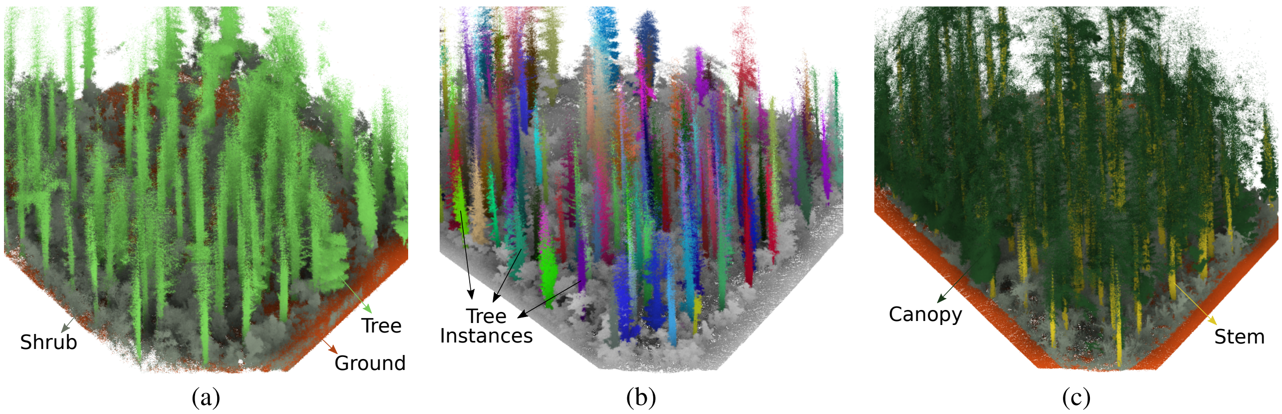

Fig. 1: We provide a longitudinal dataset of multiple forest plots, called *DigiForests*, recorded with a mobile LiDAR scanning system. The data has been recorded in three different seasons, Spring, Autumn, and Summer, with distinct vegetation appearances. Besides a semantic annotation of data into tree, shrub, and ground shown in (a), we provide instance annotations for trees shown in (b), and fine-grained annotations of stem and canopy of trees shown in (c). The depicted point clouds are merged from multiple scans. Best viewed in color.

***Abstract*— Forests are vital to our ecosystems, acting as carbon sinks, climate stabilizers, biodiversity centers, and wood sources. Due to their scale, monitoring and managing forests takes a lot of work. Forestry robotics offers the potential for enabling efficient and sustainable foresting practices through automation. Despite increasing interest in this field, the scarcity of robotics datasets and benchmarks in forest environments is hampering progress in this domain. In this paper, we present a real-world, longitudinal dataset for forestry robotics that enables the development and comparison of approaches for various relevant applications, ranging from semantic interpretation to estimating traits relevant to forestry management. The dataset consists of multiple recordings of the same plots in a forest in Switzerland during three different growth periods. We recorded the data with a mobile 3D LiDAR scanning setup. Additionally, we provide semantic annotations of trees, shrubs, and ground, instance-level annotations of trees, as well as more fine-grained annotations of tree stems and crowns. Furthermore, we provide reference field measurements of traits relevant to forestry management for a subset of the trees. Together with the data, we also provide open-source baseline panoptic segmentation and tree trait estimation approaches to enable the community to bootstrap further research and simplify comparisons in this domain.**

The author is with: [1]Center for Robotics, University of Bonn, Germany, [2]University of Oxford, UK, [3]Technical University of Munich, Germany, [4]PreFor Oy, Finland, [5]Swiss Federal Institute for Forest, Snow and Landscape Research, Switzerland, [6]Lamarr Institute for Machine Learning and Artificial Intelligence, Germany. * indicates equal contribution.

This work has been funded by the European Union's Horizon Europe research and innovation programme under grant agreement No 101070405 (DigiForest), by the Deutsche Forschungsgemeinschaft (DFG, German Research Foundation) under Germany's Excellence Strategy, EXC-2070 – 390732324 – PhenoRob and by the Swiss State Secretariat for Education, Research and Innovation (SERI).

I. Introduction

Forests are key elements of our ecosystems [16] as they support critical processes like carbon sequestration and biodiversity while also providing resources for industries and offering opportunities for human leisure [16], [34]. Preserving such important ecosystems is essential.

Foresters need precise information about forests to make effective and informed decisions on forestry management that potentially materialize only in the coming decades. Such information includes tree counts, species, and essential geometric traits such as the "diameter at breast height", or DBH, which constitute a standard forest inventory. Traditionally, humans perform labor and time-intensive field experiments to collect tree-by-tree measurements in sample plots, which are then aggregated to plot-level means and totals [27]. The prospect of forestry robotics is the automation of this data collection, monitoring, and trait computation at a larger scale than traditionally possible, potentially realizing even automated maintenance [20] and tree harvesting in the future. Foresters could then use such detailed inventories to make forecasts of stand growth, plan harvesting strategies, optimize species rotation cycles, and more, contributing to effective and sustainable foresting practices [22], [37].

Despite increasing interest in forestry robotics, only a few real-world robotics datasets and benchmarks are available in this important domain. This makes the development of new techniques and the comparison to existing ones difficult. Realistic, domain-specific datasets are often a crucial foundation for developing innovative solutions as they provide

TABLE I: Dataset characteristics of LiDAR-based forest datasets. "Sensors" lists for each dataset the primary LiDAR sensor that can be used for investigating semantic interpretation and tree trait estimation. "Meta Data" lists the availability of tree traits in the dataset.

Name	Sensors	Tree Count	Number of Classes	Tree Instances	Multi-Session	Meta Data
WildScenes [44]	Velodyne VLP-16 (MLS)	N/A	15	-	✓	-
TreeScope [8]	Ouster OS1-64 (UAV) Ouster OS0-128 (MLS)	N/A	2	-	-	✓
FOR-Instance [40]	Riegl MiniVUX-1 (UAV) Riegl VUX-1 (UAV)	1,130	5	✓	-	✓
DigiForests (Ours)	Hesai XT32 (MLS) Hesai QT64 (MLS)	2,526	5	✓	✓	✓

novel challenges and characteristics that cannot be efficiently solved by off-the-shelf solutions [1], [2], [47]. Such datasets allow researchers to investigate research questions on a common basis and compare different approaches.

In the past decade, forestry monitoring has increasingly relied on LiDAR point clouds acquired with terrestrial laser scanners (TLS) [27], [46] or airborne laser scanning [40]. This work targets data acquisition with a sensor setup enabled by conventional LiDAR scanners commonly used in robotics. They can be carried easily by a robot or be integrated into a sensor backpack. Furthermore, it does not require trained personnel to properly place a TLS or pilot a drone. Compared to TLS, such LiDAR sensors are often inferior in terms of accuracy and density of measurements. However, they are more affordable and more flexible in terms of mobility, allowing for significantly larger spatial coverage than TLS. Compared to airborne scanning, they also enable capturing important below-canopy trunk detail that can be used for estimating essential parameters like DBH, a parameter considered the most crucial in forestry [27].

This paper aims to change this current situation and provides a longitudinal dataset for forestry robotics. We provide LiDAR data recorded in real forests over extended periods of time with commonly used LiDAR sensors employed in robotics. Together with the raw data, we provide semantic annotations, tree trait reference data, and two open-source baseline implementations. This enables the investigation of LiDAR-based semantic and panoptic segmentation approaches, as well as tree trait estimation approaches in forestry environments. An example of the annotations in the dataset is shown in Fig. 1.

The main contribution of this paper is a new, longitudinal forestry dataset using robotic LiDAR sensors. We provide the raw LiDAR scans as well as locally aggregated point clouds of forest plots recorded multiple times across different seasons. The repeated measurements of the same plots are spatially aligned in a common reference frame, furthermore enabling the potential to study long-term mapping [29] and semantic interpretation in unstructured, cluttered, and changing environments. The chosen forest in Switzerland also provides a challenging application due to its wide variation of environmental characteristics (e.g., from flat to steep terrain), forest stands (e.g., conifers, mixed and broadleaf forests) and silvicultural management practices (e.g., even-aged and uneven-aged forests). To the best of our knowledge, this is the first dataset that allows for investigating panoptic segmentation in real forestry environments using commercial robotics LiDARs.

In summary, we provide: (i) a longitudinal forest dataset recorded using common robotics sensors in three different growth periods that are spatially aligned in a common reference frame, (ii) semantic annotations of point clouds that include high-level semantics of tree, shrub, and ground, instance-level annotations of the trees, fine-grained semantics of stem and canopy, and reference measurements of tree traits by domain experts in forestry, (iii) panoptic segmentation baseline as well as a tree trait estimation approach as an open source package to further bootstrap research in this domain. Complementary to the data, we provide a public semantic interpretation benchmark. The evaluation is carried out on a benchmark server with a hidden test set enabling the unbiased comparison of approaches targeted at performing tasks relevant for forestry robotics. Our dataset is available at: `https://www.ipb.uni-bonn.de/data/digiforest-dataset`, and the baselines are available at: `https://github.com/PRBonn/digiforests`.

II. Related Work

Datasets and associated benchmarks are the driver of innovation and reproducible research in robotics and computer vision. Seminal datasets [10], [12], [18], [28] allowed to push the boundaries of image-based semantic interpretation, and enabled to measure quantitatively the progress in the field. Datasets targeted specifically at perception in robotics [3], [6], [11], [30], [41], [49] laid the foundation for developing innovative approaches for LiDAR-based perception.

With growing interest in forestry robotics, there have been an increasing number of domain-specific datasets acquired in forests [8], [14], [40], [44]. Besides datasets for tree instance segmentation based on camera images [14], also datasets using LiDAR sensors have been published [8], [40], [44]. More specifically, the WildScenes dataset [44] provides repetitive trajectories of the same forest roads with semantic annotations of LiDAR points projected from image-based annotations. TreeScope [8] provides LiDAR data recorded with UAV and mobile laser scanning platforms with tree stems semantically annotated on range images. While they do provide point clouds of individual trees for evaluating DBH estimation approaches, they do not provide instance labels in a LiDAR map to evaluate instance segmentation approaches. Lastly, FOR-Instance [40] provides aerial LiDAR

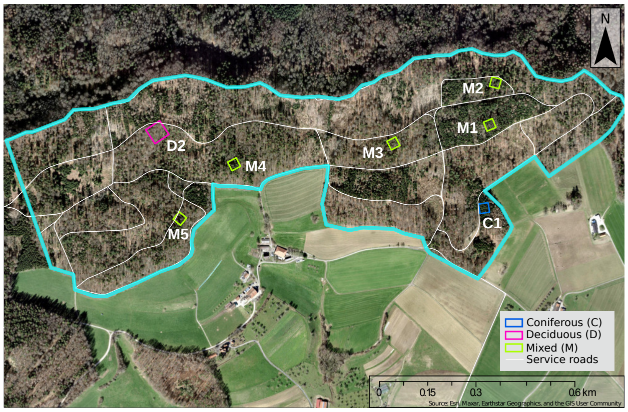

Fig. 2: Overview of the forests near Stein am Rhein, Switzerland with the different plots that we recorded in our field trials of the EU-funded project "DigiForest".

Fig. 3: For the DigiForests dataset, we recorded data with a (left) backpack-carried sensor payload in (right) challenging forest environments with the sensor payload highlighted in red (right).

data with semantic and instance annotations of point clouds with multiple measurement campaigns in different forests. They also distinguish so-called woody and live branches but note that this distinction was quite challenging in their data. While these datasets allow investigating challenging problems in forestry robotics, WildScenes, for example, does not include labels for tree instances or tree meta data which could be used for exploring panoptic segmentation or tree trait estimation approaches. While the FOR-Instance dataset provides this, the data is collected with a UAV piloted above the tree canopy, which can miss important tree trunk detail.

For forestry monitoring, several statistics are essential for making forestry management decisions, e.g., in terms of planting, thinning and harvesting. Among the most essential characteristics are the tree species and the diameter at breast height (DBH), but also economic factors like merchantable stem length, first branch height, number of bends, which determine the quality of cut wood. For tree counts and determining the position of trees, a tree instance segmentation [39], [42] using geometric [31], [39] or learning-based approaches [19] can be employed. Most approaches for DBH estimation [15], [31] employ cylinder or circle fitting to tree instance segmentation at a height of 1.3 m above ground.

In contrast to the aforementioned datasets for forestry environments, summarized in Tab. I, we provide with DigiForests a unique combination of characteristics that shows complete semantic annotations with tree instance annotations of data acquired with a robotics LiDAR sensor moving through real forests. We also provide a fine-grained annotation of stems and canopy, and a spatially consistent temporal dataset with reference field measurements conducted by domain experts.

III. A Dataset for Forestry Robotics

Our dataset was collected during multiple visits of the same sites in a forest near Stein am Rhein, Switzerland. We provide the raw data consisting of ROS bags of all data collection campaigns, but also provide post-processed aggregated scans that we annotated with labels relevant in forestry robotics applications.

In this section, we describe the data collection including the reference field measurements and the post-processing to generate the aggregated LiDAR point clouds. Furthermore, we provide insights into the labeling process, which we performed directly on the aggregated point clouds to ensure high annotation quality on the data that we envision to be used for testing semantic interpretation approaches. Lastly, we summarize the statistics about our annotations to provide a better impression of the provided data.

A. Data Collection

All data has been collected in a forest near Stein am Rhein, Switzerland, where forestry experts selected several plots that show different levels of complexity in terms of traversability and clutter, but also differ in forest types, species and silvicultural management regimes.

Thus, the selected forest stands are either conifer-dominated (e.g., spruce and larch), broadleaf-dominated (e.g., beech), or mixed (e.g., linden, pine and larch), and the regeneration and ground coverage with vegetation varies from sparse and low to dense and high. Fig. 2 shows a map visualization where individual plots are identified by a plot number prefixed by a letter corresponding to the most dominant tree family, i.e., "D" for deciduous, "C" for coniferous, and "M" for mixed plots with both kinds of trees.

We collected data in different growth periods, specifically: March 2023, October 2023, and July 2024. The data was collected with a backpack mounted sensor package consisting of a Hesai XT32 LiDAR inclined at 45 degrees (March 2023), and a Hesai QT64 horizontally aligned (October 2023). In July 2024, we collected data with a combination of a horizontally aligned Hesai QT32 and a Hesai XT32 inclined at 45 degrees to ensure maximum coverage of the tree stems and tree canopy. The sensor package was additionally equipped with a GNSS receiver for geo-referencing the data and multiple cameras were employed for visual odometry. Detailed specifications of our sensor package are available on the website for our dataset.

Additionally, for the March 2023 and July 2024 campaigns we used a UAV-mounted Velodyne HDL-32E and Hesai XT-32M2X respectively to record aerial data offering better canopy representation covering the entire forest region shown in Fig. 2. This aerial data was aligned with the data from the backpack Hesai sensors following the methodology of Casseau et al. [7] and is also provided in this dataset.

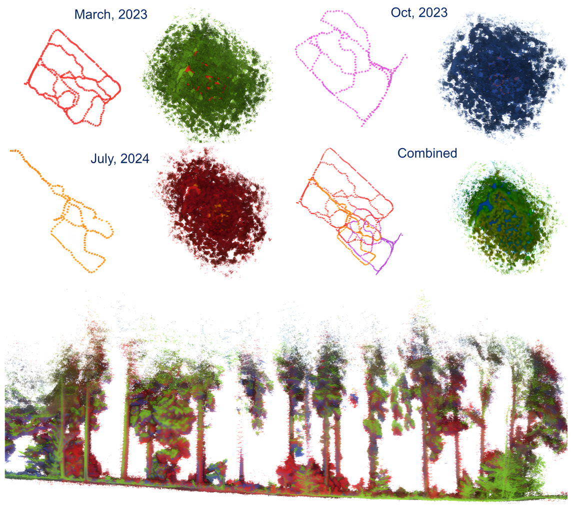

Fig. 4: (Top) Visualization of spatially aligned trajectories for the M2 plot. (Bottom) Side view of the combined point cloud from three data collection sessions showing accurate co-registration. Green, blue and red points correspond to scans from March 2023, October 2023 and July 2024 missions respectively.

Reference measurements were carried out during the March 2023 campaign. We tagged individual trees with AprilTags [36] to ease the process of associating the manual measurements with the recorded data by automatic detection of the AprilTags using the camera streams (see Fig. 3). Forestry experts from the Swiss Federal Institute for Forest, Snow, and Landscape Research (WSL) conducted manual measurements of tree DBH, length of clear wood, height of first green branch, tree species and more, allowing a tree-specific data association through the AprilTags. This forest inventory is provided along with the rest of the dataset.

We provide also the raw data collected during these field campaigns as we see opportunities to use the data to investigate LiDAR odometry in unstructured environments, which is challenging for conventional LiDAR odometry approaches working well in the context of urban environments [45]. In particular, the high-frequency motion profile of a backpack-carried sensor combined with the limited field of view inside the forest due to occlusions poses a challenge for LiDAR-only approaches. Loop closure detection is also challenging in forests [35], where domain-specific approaches could provide more robust and accurate results.

B. Post-Processing

The collected data was post-processed to generate aggregated point cloud maps, enabling semantic interpretation and trait estimation approaches to work with data completely covering the stem region of trees. We aligned the recorded data using a pose graph optimization, fusing LiDAR, IMU, and visual odometry to recover the trajectory walked in the forests. For this purpose, we employed VILENS [48] to recover individual per-plot trajectories and provide the poses generated by VILENS in addition to the raw data.

A key contribution of our dataset is the spatial alignment of trajectories and point clouds across seasons. To achieve sequence-to-sequence alignment across different data

TABLE II: Statistics of number of trees annotated for all plots.

Plot	Number of trees		
	Mar 2023	Oct 2023	Jul 2024
C1	275	130	166
D2	157	159	156
M1	256	-	-
M2	95	137	157
M3	229	-	-
M4	388	-	-
M5	221	-	-
Sum	1,621	426	479

collection seasons, we jointly optimized a pose graph over an individual plot's trajectories from all sessions, globally aligning all point clouds spatially. A crucial step in this process involved identifying loop closures between different sessions using Logg3dNet [43], which demonstrated reliable and robust performance in forestry environments [35]. Fig. 4 illustrates the result of spatial alignment for plot M2.

C. Annotation

For annotation, we manually labeled and verified all sequences using an extension of a point cloud annotation tool developed originally for creating the SemanticKITTI dataset [4]. We extended the tool to label tree instances directly to allow an accurate labeling of the unstructured and cluttered forest environments. Labeling forest scenes was more challenging than annotating urban environments and the labeling time depended heavily on the amount of trees visible in a recording. To speed up labeling, we employed a cloth simulation-based ground filtering [50] that allowed to obtain an initial ground segmentation. Later, we manually corrected the automatic ground segmentation to ensure high quality of ground labels. For tree annotation, we concentrated on larger trees with thick stems, which are also more relevant for forestry operations and harvesting. We also labeled for each tree instance the stem and canopy points. Both classes are important for estimating traits, like DBH and crown volume, which are crucial for forest stand growth studies and forest ecology [21]. Near-ground vegetation in the scene was assigned the shrub label.

Data was recorded across three different seasons and we first focused on labeling the March 2023 session of the data. Where possible we exploited the spatial alignment of the LiDAR data detailed in Sec. III-B to transfer labels from one timestamp to another via nearest neighbor assignment. This produced a coarse labeling of data for October 2023 and July 2024, where we performed an additional round of labeling to ensure complete and accurate annotations, especially for parts where the vegetation had changed across seasons.

Overall, we provide annotated point cloud data for seven plots collected in March 2023, October 2023, and July 2024. In Tab. II, we provide plot-wise statistics of the number of annotated trees. In total, we annotated 2,526 trees. We provide for all reference trees of the March 2023 data individual reference measurements of tree species, DBH, length of clear wood, height of first green branch, and also qualitative measures such as number of bends, dead limbs, and condition of the crown (e.g., broken top, crown defects), which were manually measured and assessed by forestry domain experts. In terms of label distribution, the annotated data contains 29.2% tree points, 24.4% shrub, 26.7% ground points, and 0.4% outlier points; 40.9% of the tree points are stem and the remaining 49.1% are canopy or foliage.

IV. Baseline Results

In this section, we present results for two essential tasks relevant in forestry robotics: LiDAR-based semantic interpretation and LiDAR-based DBH trait estimation. We present results with off-the-shelf commonly employed approaches as well as a purpose-fit approach which we have open-sourced as a baseline to further bootstrap research in this domain.

A. Semantic Interpretation

For this task, we evaluate the performance of several approaches that perform semantic, instance or panoptic segmentation. In our case, the ground and shrub classes are treated as stuff classes [24] for panoptic segmentation, while the tree class has instances and is treated as a thing class.

For reproducible results, we split the data in DigiForests (see Tab. II) into the following proportions. For training, we use the full temporal sequence (March 2023, October 2023, July 2024) for plot D2, and plots M1, M3, M4, M5 from the March 2023 data. For validation, i.e., selection of hyperparameters, we use the full temporal sequence of plot C1. For testing, we use the full temporal sequence from plot M2. This selection leads to a clear separation of recording locations across the three splits and for the test set to see a mixture of tree species and distributions, allowing to test the generalization performance of trained models. In summary, we have 7 plots for training, 3 plots for validation, and 3 plots as test set, with each set including one full temporal sequence of data.

Our dataset contains semantic labels for ground, shrub, and tree points and also instance labels for tree points. Tree points further can have semantic labels for stem or canopy. Hence, our dataset uniquely lends itself to investigate multiple different problems in the wider context of semantic interpretation of forest scenes using commercial rotating LiDARs. We therefore tested a mix of recent approaches for semantic, instance and panoptic segmentation from both the wider automated driving domain and the more adjacent agricultural domain. Following established protocols [3], [33], [44], and given the mix of approaches we tested, where possible we report the standard intersection-over-union (IoU) metric for performance on semantic classes and mean IoU (mIoU) for overall semantic segmentation performance. For evaluating panoptic segmentation performance, we use the panoptic quality metric [24], [38], where the per-class panoptic quality PQ_c is given by

$$\text{PQ}_c = \begin{cases} \dfrac{\sum_{(p,g)\in\text{TP}} \text{IoU}(p,g)}{|\text{TP}| + \frac{1}{2}|\text{FP}| + \frac{1}{2}|\text{FN}|} & \text{, if } c \text{ is thing} \\ \text{IoU}(p,g) & \text{, if } c \text{ is stuff} \end{cases}, \quad (1)$$

where p refers to the predicted and g to the ground truth segments of class c, TP is the set of true positives, FP is the set of false positives, FN is the set of false negatives, and $|\cdot|$ represents the cardinality of the set. For thing classes, we follow the definition by Kirillov et al. [23] for data association of instance segments. Each predicted segment p is assigned to the ground truth segment g if its IoU is greater than 0.5 and is added to TP. Predicted instances p without a matching ground truth segment are added to FP and ground truth segments g without an associated prediction are added to FN. For stuff classes, we follow the implementation by Behley et al. [5] and compute simply the IoU between all points p assigned to class c and the points g with class c in the ground truth. As defined in Eq. (1), this renders PQ_c for stuff classes the same as its IoU which allows easier comparison between purely semantic and panoptic segmentation approaches. The overall panoptic quality PQ over all classes $\mathcal{C}$, i.e., ground, tree, and shrub, are given by the average over class-wise panoptic qualities given by:

$$\text{PQ} = \frac{1}{|\mathcal{C}|} \sum_{c\in\mathcal{C}} \text{PQ}_c \,. \quad (2)$$

We trained multiple off-the-shelf promising baselines and also implemented a purpose-fit approach for semantic interpretation on our DigiForests dataset. For all approaches, we report the relevant metrics on the test set in Tab. III. For reproducibility, we provide the scripts to compute the metrics based on the ground truth and predictions by segmentation approaches. First, from the automated driving domain, we trained the range-image based approach by Fusaro et al. [17] as a semantic segmentation baseline. We used the ground, shrub, stem, and canopy labels as the target semantic classes, and report the IoU and the mIoU across these classes. Then, we trained the approach by Marks et al. [33], an effective approach from the agricultural domain for instance segmenting leafs on plants. We adapted it to perform instance segmentation of the trees. Similar to how they report PQ on the leaf class in their work, we report here the PQ on just the tree class. We additionally trained the transformer-based MaskPLS by Marcuzzi et al. [32] developed to perform panoptic segmentation in the automated driving domain. MaskPLS predicts a set of non-overlapping binary masks, each representing a single instance belonging to either a thing or a stuff class. It cannot segment a tree instance also for stem and canopy simultaneously. Hence, we train it using ground, shrub and tree as target labels and report the IoU for ground and shrub, PQ_{tree} for tree, and mean PQ across the three classes as defined by Eq. (1) and Eq. (2).

We also implemented our own approach for panoptic segmentation while also designing it to be capable of both fine-grained stem-canopy and tree instance segmentation. We report the results of our approach in Tab. III as "Forest Pan. Seg.". Our network consists of a MinkUNet [9] backend using sparse spatial convolutions with 790k parameters producing a feature embedding per point. We then pass the embedding through two network heads: a semantic segmentation head to predict either ground, shrub, stem or canopy, and

TABLE III: Results for semantic interpretation on the test set of DigiForests. For stuff classes, IoU is equivalent to PQ_c as defined by Eq. (1). mIoU is computed considering the ground, shrub, stem and canopy classes. PQ is computed considering the ground, shrub, and tree classes. We implemented our own approach for panoptic segmentation, reported here as "Forest Pan. Seg."

Approach	IoU				mIoU	PQ_{tree}	PQ
	Ground	Shrub	Stem	Canopy			
Fusaro et al. [17]	79.4	66.0	42.6	12.8	50.2	-	-
Marks et al. [33]	-	-	-	-	-	53.1	-
Marcuzzi et al. [32]	65.9	53.9	-	-	-	57.0	58.9
Forest Pan. Seg. (Ours)	**79.5**	**72.7**	**78.5**	**48.2**	**69.7**	**57.8**	**70.0**

an offset vector prediction head which produces a per-point offset vector to the center of the instance a point belongs to. We then generate a tree mask using the predicted stem and canopy semantics, add the predicted offset vectors just to the points falling in the tree mask, and cluster the shifted tree points using DBSCAN [13] to produce an instance segmentation of trees. With this, our approach is capable of ground, shrub, stem, and canopy segmentation and also tree instance segmentation. From Tab. III, we see that our approach outperforms all other baselines on semantic and panoptic segmentation metrics.

B. DBH Trait Estimation

Tree diameter at breast height is widely considered the most crucial parameter in forestry [27]. As part of our DigiForests dataset, we provide a forest inventory for trees from the March 2023 session which also includes DBH. Common approaches for DBH estimation perform either circle [39] or cylinder fitting [42], considering that either a manual segmentation of trees is available [42] or segmenting the trees as part of their approach as well [31]. We report baseline DBH estimation results of several approaches in Tab. IV. To evaluate an approach, each tree in the known ground truth is assigned to the closest predicted tree location using a nearest neighbor search on the tree position and a maximum search radius of 0.7 m. As metrics, we use the recall of inventory trees reconstructed and RMSE of their estimated DBH. We report these values as "Plot Avg." by averaging the results across each plot [26], [27] and as "Total" by considering all trees in the inventory.

We first report the results of the approach by Freißmuth et al. [15], an online approach for tree DBH estimation capable of operating at sensor frame rate. Then, we report the results of the approach from Krisanski et al. [25], a deep-learning based approach for tree segmentation and geometric DBH estimation. Next, we use our panoptic segmentation approach detailed in Sec. IV-A to obtain just a stem cloud and then follow the methodology of Malladi et al. [31] to fit cylinders to the stems. The results of our DBH estimation are reported as "For. Pan. Seg. + Cyl. Fit." in Tab. IV. Finally, we use ground truth annotations directly to obtain the stem cloud and repeat the cylinder fitting methodology as above. The result of this is reported as "G.T. + Cyl. Fit." in Tab. IV.

From the results, we see that the approach of Freißmuth et al. [15] achieves the best RMSE of the evaluated methods, but has a lower recall compared to other methods. The approach is an online method and might fail in reconstructing

TABLE IV: Results for tree DBH estimation on DigiForests. RMSE is reported in cm.

Approach	Plot Avg. Recall	Total Recall	Plot Avg. RMSE	Total RMSE
Freißmuth et al. [15]	0.88	0.92	3.42	3.15
Krisanksi et al. [25]	0.98	0.98	6.10	7.43
Forest Pan. Seg. + Cyl. Fit.	0.98	0.98	5.32	6.41
G.T. + Cyl. Fit.	0.98	0.98	3.55	4.04

challenging trees, whereas the others are offline and thus have the chance to perform better in such scenarios. The approach by Krisanski et al. [25] is indeed better in recall. Using "Forest Pan. Seg." followed by cylinder fitting performs similar to Krisanski et al. [25] in recall and outperforms them in terms of RMSE. Comparing the results of using ground truth annotations followed by cylinder fitting, we see that, as expected, the quality of stem segmentation itself influences the performance of DBH estimation. Better results can therefore be obtained by first improving the segmentation results in the pipeline. Futhermore, more sophisticated geometric primitives for estimating DBH can be explored. We do however note that, from earlier studies [26], [27], the accuracy of DBH estimation using even TLS sensors typically falls within the range of 1 to 4 cm.

V. Conclusion

In this paper, we presented DigiForests, a novel dataset providing longitudinal data of forestry environments for robotics research. Together with the data recorded with a backpack-carried rotating LiDAR sensor frequently used in robotics, we provide annotated point clouds that allow to investigate semantic interpretation and tree trait estimation in forestry. The provided data is complemented by a semantic interpretation benchmark, where we provide server-sided evaluation on a hidden test set enabling the unbiased comparison of approaches targeted at performing tasks relevant for forestry robotics. We report the performance of several off-the-shelf approaches and also open source a purpose-fit approach which can be used to bootstrap further research.

Besides the presented applications, we see the prospect to investigate with this data further tasks, such as LiDAR-based odometry in unstructured environments, better approaches for loop closure, and temporal data association to enable the tracking of traits for forestry monitoring applications.

Acknowledgments

We thank Benedikt Mersch for valuable discussions when implementing our segmentation approach. We also thank Holger Griess for installing the field plots.

References

[1] B. Bazzana, H. Andreasson, and G. Grisetti. How-to augmented lagrangian on factor graphs. *IEEE Robotics and Automation Letters (RA-L)*, 9(3):2806–2813, 2024.

[2] B. Bazzana, T. Guadagnino, and G. Grisetti. Handling constrained optimization in factor graphs for autonomous navigation. *IEEE Robotics and Automation Letters (RA-L)*, 8(1):432–439, 2023.

[3] J. Behley, M. Garbade, A. Milioto, J. Quenzel, S. Behnke, J. Gall, and C. Stachniss. Towards 3D LiDAR-based Semantic Scene Understanding of 3D Point Cloud Sequences: The SemanticKITTI Dataset. *Intl. Journal of Robotics Research (IJRR)*, 40(8–9):959–967, 2021.

[4] J. Behley, M. Garbade, A. Milioto, J. Quenzel, S. Behnke, C. Stachniss, and J. Gall. SemanticKITTI: A Dataset for Semantic Scene Understanding of LiDAR Sequences. In *Proc. of the IEEE/CVF Intl. Conf. on Computer Vision (ICCV)*, 2019.

[5] J. Behley, A. Milioto, and C. Stachniss. A Benchmark for LiDAR-Based Panoptic Segmentation Based on KITTI. In *Proc. of the IEEE Intl. Conf. on Robotics & Automation (ICRA)*, 2021.

[6] H. Caesar, V. Bankiti, A. Lang, S. Vora, V. Liong, Q. Xu, A. Krishnan, Y. Pan, G. Baldan, and O. Beijbom. nuScenes: A Multimodal Dataset for Autonomous Driving. In *Proc. of the IEEE/CVF Conf. on Computer Vision and Pattern Recognition (CVPR)*, 2020.

[7] B. Casseau, N. Chebrolu, M. Mattamala, L. Freissmuth, and M. Fallon. Markerless Aerial-Terrestrial Co-Registration of Forest Point Clouds using a Deformable Pose Graph. In *Proc. of the IEEE/RSJ Intl. Conf. on Intelligent Robots and Systems (IROS)*, 2024.

[8] D. Cheng, F.C. Ojeda, A. Prabhu, X. Liu, A. Zhu, P.C. Green, R. Ehsani, P. Chaudhari, and V. Kumar. TreeScope: An Agricultural Robotics Dataset for LiDAR-Based Mapping of Trees in Forests and Orchards. *arXiv preprint*, arXiv:2310.02162, 2023.

[9] C. Choy, J. Gwak, and S. Savarese. 4D Spatio-Temporal ConvNets: Minkowski Convolutional Neural Networks. In *Proc. of the IEEE/CVF Conf. on Computer Vision and Pattern Recognition (CVPR)*, 2019.

[10] M. Cordts, S.M. Omran, Ramos, T. Rehfeld, M. Enzweiler, R. Benenson, U. Franke, S. Roth, and B. Schiele. The cityscapes dataset for semantic urban scene understanding. In *Proc. of the IEEE Conf. on Computer Vision and Pattern Recognition (CVPR)*, 2016.

[11] A. Dai, A. Chang, M. Savva, M. Halber, T. Funkhouser, and M. Nießner. ScanNet: Richly-Annotated 3D Reconstructions of Indoor Scenes. In *Proc. of the IEEE Conf. on Computer Vision and Pattern Recognition (CVPR)*, 2017.

[12] J. Deng, W. Dong, R. Socher, L. Li, K. Li, and L. Fei-Fei. Imagenet: A large-scale hierarchical image database. In *Proc. of the IEEE Conf. on Computer Vision and Pattern Recognition (CVPR)*, 2009.

[13] M. Ester, H. Kriegel, J. Sander, and X.Xu. A density-based algorithm for discovering clusters in large spatial databases with noise. In *Proc. of the Conf. on Knowledge Discovery and Data Mining (KDD)*, 1996.

[14] J.M. Fortin, O. Gamache, V. Grondin, F. Pomerleau, and P. Giguere. Instance Segmentation for Autonomous Log Grasping in Forestry Operations. In *Proc. of the IEEE/RSJ Intl. Conf. on Intelligent Robots and Systems (IROS)*, 2022.

[15] L. Freißmuth, M. Mattamala, N. Chebrolu, S. Schaefer, S. Leutenegger, and M. Fallon. Online Tree Reconstruction and Forest Inventory on a Mobile Robotic System. In *Proc. of the IEEE/RSJ Intl. Conf. on Intelligent Robots and Systems (IROS)*, 2024.

[16] P.D. Frenne, J. Lenoir, M. Luoto, B.R. Scheffers, F. Zellweger, J. Aalto, M.B. Ashcroft, D.M. Christiansen, G. Decocq, K.D. Pauw, S. Govaert, C. Greiser, E. Gril, A. Hampe, T. Jucker, D.H. Klinges, I.A. Koelemeijer, J.J. Lembrechts, R. Marrec, C. Meeussen, J. Ogée, V. Tyystjärvi, P. Vangansbeke, and K. Hylander. Forest microclimates and climate change: Importance, drivers and future research agenda. *Global Change Biology*, 27(11):2279–2297, 2021.

[17] D. Fusaro, S. Mosco, E. Menegatti, and A. Pretto. Exploiting local features and range images for small data real-time point cloud semantic segmentation. In *Proc. of the IEEE/RSJ Intl. Conf. on Intelligent Robots and Systems (IROS)*, 2024.

[18] A. Geiger, P. Lenz, and R. Urtasun. Are we ready for Autonomous Driving? The KITTI Vision Benchmark Suite. In *Proc. of the IEEE Conf. on Computer Vision and Pattern Recognition (CVPR)*, 2012.

[19] V. Grondin, J.M. Fortin, F. Pomerleau, and P. Giguere. Tree detection and diameter estimation based on deep learning. *Forestry: An International Journal of Forest Research*, 96(2):264–276, 2023.

[20] T. Guadagnino, B. Mersch, I. Vizzo, S. Gupta, M.V. Malladi, L. Lobefaro, G. Doisy, and C. Stachniss. Kinematic-ICP: Enhancing LiDAR Odometry with Kinematic Constraints for Wheeled Mobile Robots Moving on Planar Surfaces. In *Proc. of the IEEE Intl. Conf. on Robotics & Automation (ICRA)*, 2025.

[21] G. Hemery, P. Savill, and S. Pryor. Applications of the crown diameter–stem diameter relationship for different species of broadleaved trees. *Forest Ecology and Management*, 215(1):285–294, 2005.

[22] S. Holm and J. Schweier. Virtual forests for decision support and stakeholder communication. *Environmental Modelling & Software*, 180:106159, 2024.

[23] A. Kirillov, R. Girshick, K. He, and P. Dollar. Panoptic Feature Pyramid Networks. In *Proc. of the IEEE/CVF Conf. on Computer Vision and Pattern Recognition (CVPR)*, 2019.

[24] A. Kirillov, K. He, R. Girshick, C. Rother, and P. Dollár. Panoptic Segmentation. In *Proc. of the IEEE/CVF Conf. on Computer Vision and Pattern Recognition (CVPR)*, 2019.

[25] S. Krisanski, M.S. Taskhiri, S.G. Aracil, D. Herries, A. Muneri, M.B. Gurung, J. Montgomery, and P. Turner. Forest structural complexity tool—an open source, fully-automated tool for measuring forest point clouds. *Remote Sensing*, 13(22), 2021.

[26] D. Kükenbrink, M. Marty, R. Bösch, and C. Ginzler. Benchmarking laser scanning and terrestrial photogrammetry to extract forest inventory parameters in a complex temperate forest. *International Journal of Applied Earth Observation and Geoinformation*, 113:102999, 2022.

[27] X. Liang, V. Kankare, J. Hyyppä, Y. Wang, A. Kukko, H. Haggrén, X. Yu, H. Kaartinen, A. Jaakkola, F. Guan, M. Holopainen, and M. Vastaranta. Terrestrial laser scanning in forest inventories. *ISPRS Journal of Photogrammetry and Remote Sensing (JPRS)*, 115:63–77, 2016.

[28] T. Lin, M. Maire, S. Belongie, J. Hays, P. Perona, D. Ramanan, P. Dollár, and C.L. Zitnick. Microsoft COCO: Common Objects in Context. In *Proc. of the Europ. Conf. on Computer Vision (ECCV)*, 2014.

[29] L. Lobefaro, M. Malladi, T. Guadagnino, and C. Stachniss. Spatio-Temporal Consistent Mapping of Growing Plants for Agricultural Robots in the Wild. In *Proc. of the IEEE/RSJ Intl. Conf. on Intelligent Robots and Systems (IROS)*, 2024.

[30] W. Maddern, G. Pascoe, C. Linegar, and P. Newman. 1 year, 1000 km: The oxford robotcar dataset. *Intl. Journal of Robotics Research (IJRR)*, 36(1):3–15, 2017.

[31] M. Malladi, T. Guadagnino, L. Lobefaro, M. Mattamala, H. Griess, J. Schweier, N. Chebrolu, M. Fallon, J. Behley, and C. Stachniss. Tree Instance Segmentation and Traits Estimation for Forestry Environments Exploiting LiDAR Data. In *Proc. of the IEEE Intl. Conf. on Robotics & Automation (ICRA)*, 2024.

[32] R. Marcuzzi, L. Nunes, L. Wiesmann, J. Behley, and C. Stachniss. Mask-Based Panoptic LiDAR Segmentation for Autonomous Driving. *IEEE Robotics and Automation Letters (RA-L)*, 8(2):1141–1148, 2023.

[33] E. Marks, M. Sodano, F. Magistri, L. Wiesmann, D. Desai, R. Marcuzzi, J. Behley, and C. Stachniss. High precision leaf instance segmentation for phenotyping in point clouds obtained under real field conditions. *IEEE Robotics and Automation Letters*, 8(8):4791–4798, 2023.

[34] A.S. Mori, K.P. Lertzman, and L. Gustafsson. Biodiversity and ecosystem services in forest ecosystems: a research agenda for applied forest ecology. *Journal of Applied Ecology*, 54(1):12–27, 2017.

[35] H. Oh, N. Chebrolu, M. Mattamala, L. Freissmuth, and M. Fallon. Evaluation and Deployment of LiDAR-based Place Recognition in Dense Forests. In *Proc. of the IEEE/RSJ Intl. Conf. on Intelligent Robots and Systems (IROS)*, 2024.

[36] E. Olson. AprilTag: A Robust and Flexible Visual Fiducial System. In *Proc. of the IEEE Intl. Conf. on Robotics & Automation (ICRA)*, 2011.

[37] L. Pellissier, M. Anzini, L. Maiorano, A. Dubuis, J. Pottier, P. Vittoz, and A. Guisan. Spatial predictions of land-use transitions and associated threats to biodiversity: the case of forest regrowth in mountain grasslands. *Applied Vegetation Science*, 16(2):227–236, 2013.

[38] L. Porzi, S.R. Bulo, A. Colovic, and P. Kontschieder. Seamless Scene Segmentation. In *Proc. of the IEEE/CVF Conf. on Computer Vision and Pattern Recognition (CVPR)*, 2019.

[39] A. Proudman, M. Ramezani, S.T. Digumarti, N. Chebrolu, and M. Fallon. Towards real-time forest inventory using handheld LiDAR. *Journal on Robotics and Autonomous Systems (RAS)*, 157:104240, 2022.

[40] S. Puliti, G. Pearse, P. Surovy, L. Wallace, M. Hollaus, M. Wielgosz, and R. Astrup. FOR-instance: a UAV laser scanning benchmark dataset

for semantic and instance segmentation of individual trees. *arXiv preprint*, arXiv:2309.01279, 2023.

[41] M. Ramezani, Y. Wang, M. Camurri, D. Wisth, M. Mattamala, and M. Fallon. The newer college dataset: Handheld lidar, inertial and vision with ground truth. In *Proc. of the IEEE/RSJ Intl. Conf. on Intelligent Robots and Systems (IROS)*, 2020.

[42] J.F. Tremblay, M. Beland, R. Gagnon, F. Pomerleau, and P. Giguere. Automatic three-dimensional mapping for tree diameter measurements in inventory operations. *Journal of Field Robotics (JFR)*, 37(8):1328–1346, 2020.

[43] K. Vidanapathirana, M. Ramezani, P. Moghadam, S. Sridharan, and C. Fookes. LoGG3D-Net: Locally guided global descriptor learning for 3D place recognition. In *Proc. of the IEEE Intl. Conf. on Robotics & Automation (ICRA)*, 2022.

[44] K. Vidanapathirana, J. Knights, S. Hausler, M. Cox, M. Ramezani, J. Jooste, E. Griffiths, S. Mohamed, S. Sridharan, C. Fookes, and P. Moghadam. WildScenes: A Benchmark for 2D and 3D Semantic Segmentation in Large-scale Natural Environments. *Intl. Journal of Robotics Research (IJRR)*, 0(0), 2024.

[45] I. Vizzo, T. Guadagnino, B. Mersch, L. Wiesmann, J. Behley, and C. Stachniss. KISS-ICP: In Defense of Point-to-Point ICP – Simple, Accurate, and Robust Registration If Done the Right Way. *IEEE Robotics and Automation Letters (RA-L)*, 8(2):1029–1036, 2023.

[46] H. Weiser, J. Schäfer, L. Winiwarter, N. Krasovec, F.E. Fassnacht, and B. Höfle. Individual tree point clouds and tree measurements from multi-platform laser scanning in german forests. *Earth System Science Data*, 14(7):2989–3012, 2022.

[47] J. Weyler, F. Magistri, E. Marks, Y.L. Chong, M. Sodano, G. Roggiolani, N. Chebrolu, C. Stachniss, and J. Behley. PhenoBench: A Large Dataset and Benchmarks for Semantic Image Interpretation in the Agricultural Domain. *IEEE Trans. on Pattern Analysis and Machine Intelligence (TPAMI)*, 46(12):9583–9594, 2024.

[48] D. Wisth, M. Camurri, and M. Fallon. VILENS: Visual, Inertial, Lidar, and Leg Odometry for All-Terrain Legged Robots. *IEEE Trans. on Robotics (TRO)*, 39(1):309–326, 2023.

[49] L. Zhang, M. Helmberger, L. Frank, T. Fu, D. Wisth, M. Camurri, D. Scaramuzza, and M. Fallon. Hilti-Oxford Dataset: A Millimetre-Accurate Benchmark for Simultaneous Localization and Mapping. *IEEE Robotics and Automation Letters (RA-L)*, 8(1):408–415, 2023.

[50] W. Zhang, J. Qi, P. Wan, H. Wang, D. Xie, X. Wang, and G. Yan. An easy-to-use airborne lidar data filtering method based on cloth simulation. *Remote Sensing*, 8(6), 2016.